SIRT6 pharmacological inhibition delays skin cancer progression in the squamous cell carcinoma

Elena Abbotto [a,1], Caterina Miro [b,1], Francesco Piacente [a], Annalisa Salis [a], Melania Murolo [b], Annarita Nappi [b], Enrico Millo [a], Eleonora Russo [c], Elena Cichero [c], Laura Sturla [a], Alberto Del Rio [d,e], Antonio De Flora [a], Alessio Nencioni [f,g,*,2], Monica Dentice [b,2], Santina Bruzzone [a,g,**,2]

[a] DIMES, Section of Biochemistry, University of Genova, Viale Benedetto XV, 1, 16132 Genova, Italy
[b] Department of Clinical Medicine and Surgery, University of Napoli Federico II, Via Pansini, 5, 80131 Napoli, Italy
[c] Department of Pharmacy, University of Genova, Viale Benedetto XV, 3, 16132 Genova, Italy
[d] Innovamol Consulting Srl, Strada San Faustino 167, 41126 Modena, Italy
[e] Institute of Organic Synthesis and Photoreactivity (ISOF), National Research Council of Italy (CNR), Via P. Gobetti 101, I-40129 Bologna, Italy
[f] Department of Internal Medicine, University of Genova, Viale Benedetto XV, 6, 16132 Genova, Italy
[g] IRCCS Ospedale Policlinico San Martino, Largo Rosanna Benzi 10, 16132 Genova, Italy

ARTICLE INFO

ABSTRACT

Sirtuin 6 (SIRT6) has a critical role in cutaneous Squamous Cell Carcinoma (cSCC): SIRT6 silencing in skin SCC cells has pro-differentiating effects and SIRT6 deletion abrogated DMBA-TPA-induced skin tumorigenesis in mice. On the other hand, SIRT6 acts as tumor suppressor in SCC by enhancing glycolysis in tumor propagating cells. Herein, pharmacological modulation of SIRT6 deacetylase activity was investigated in cSCC, with S6 (inhibitor) or MDL-800 (activator). In cSCC cells, S6 recreated the pro-differentiating effects of SIRT6 silencing, as the levels of Keratin 1, Keratin 10 and Loricrin were upregulated compared to controls. Next, the effects of SIRT6 pharmacological modulation were evaluated in a DMBA-TPA-induced skin cancer mouse model. Mice treated with the inhibitor S6 in a preventive approach, i.e. at the beginning of the promotion stage, presented reduced number and size of papillomas, compared to the controls. The epidermal hyperproliferation marker Keratin 6 and the cSCC marker Keratin 8 were less abundant when SIRT6 was inhibited. In S6-treated lesions, the Epithelial-Mesenchymal Transition (EMT) markers Zeb1 and Vimentin were less expressed compared to un-treated lesions. In a therapeutic approach, i.e. treatment starting after papilloma appearance, the S6 group presented reduced papillomas (number and size), whereas MDL-800-treated mice displayed an opposite trend. In S6-treated lesions, Keratin 6 and Keratin 8 were less expressed, EMT was less advanced, with a higher E-cadherin/Vimentin ratio, indicating a delayed carcinogenesis when SIRT6 was inhibited. Our results confirm that SIRT6 plays a role in skin carcinogenesis and suggest SIRT6 pharmacological inhibition as a promising strategy in cSCC.

1. Introduction

Cutaneous Squamous Cell Carcinoma (cSCC) is classified as non-melanoma skin cancer (NMSC) and together with Basal Cell Carcinoma (BCC) represents the most common type of cancer worldwide [1].

cSCC generally appears as a firm, red nodule, as an open soar or as a flat lesion with a scaly, crusted surface. It usually arises on sun-exposed areas of the body, but it can also develop elsewhere. If left untreated, cSCC can eventually metastasize, mainly to the liver, lungs and lymph nodes [2]. The available treatment options for localized cSCC include surgery, cryotherapy and Photo-Dynamic Therapy, with surgery being the most common and effective therapy used [2]. However, these cures do not always prove effective, and tumor relapses often occur. Apart from creams containing either 5-Fluorouracil, Celecoxib, or Imiquimod, no other drugs are used to topically treat cSCC [3]. Thus, novel and effective medications are needed to treat patients, especially those who relapse after surgery or those presenting with numerous, synchronous, cancerous or pre-cancerous lesions (field cancerization).

Sirtuins (SIRTs) are a family of evolutionary conserved enzymes that require nicotinamide adenine dinucleotide (NAD$^+$) as co-substrate to deac(et)ylate target proteins. In mammals the 7 known sirtuins, named SIRT1 to SIRT7, are classified as class III histone deacetylases (HDACs). Their substrates also include non-histone proteins, such as cytoskeletal proteins, signalling molecules, transcription factors, chaperones, p53 and DNA repair proteins [4]. Sirtuins are characterized by diverse sub-cellular localizations, unique substrate specificity, distinct enzymatic activities and different tissue abundancy [4,5] and this confers to each isoform specific functions. Given their involvement in different biological pathways, ranging from transcription to metabolism and to genome stability [4], their dysregulation is implicated in many diseases, such as cancer, neurodegenerative disorders, diabetes mellitus, cardio-vascular and autoimmune diseases [6].

In cancer, sirtuins often possess a dual and in some cases controversial function, behaving as oncopromoter or oncosuppressor, depending on the sirtuin and on the cancer type and/or stage [7]. Sirtuins have been found to be implicated in a variety of skin-specific cellular functions and processes and sirtuins' dysregulation has been observed in many skin-related diseases, including psoriasis, melanoma, cSCC and BCC [8]. In cSCC, all sirtuins are upregulated (by 3- to 16- fold) compared to normal skin epithelium, both at the mRNA and at the protein level [9–11]. The role of sirtuins in cSCC pathophysiology has only been addressed for some of these enzymes, i.e. SIRT1, SIRT2 and SIRT6 [9, 11–15].

SIRT6 is a mainly nuclear sirtuin and its role in human physiology and disease is being increasingly recognized, covering many different functions, including energy metabolism derived both from glucose and lipids, DNA repair, aging, inflammation and immunity [16,17]. SIRT6 contributes to double-strand break repair and to telomere maintenance by means of multiple mechanisms [18]. SIRT6 regulates glucose homeostasis by inhibiting different glycolytic genes, while mitochondrial respiration is enhanced [19]. Also, SIRT6 blocks IGF-AKT signaling, and, by deacetylating the Acetyltransferase GCN5 (General Control Non-repressed Protein 5), it modulates the acetylation levels of PGC-1α, which is a master regulator of mitochondrial biogenesis and a modulator of gluconeogenesis [20]. In addition, SIRT6 represses the transcription of the sterol regulatory element binding proteins 1 and 2 (SREBP1 and SREBP2) genes, reducing cholesterol levels and protecting against the physiological damage of obesity [21].

The function of SIRT6 in cancer is likely tissue specific, acting as a tumor suppressor or rather, to promote tumorigenesis depending on the cancer type. The increased SIRT6 levels in human SCC suggests that SIRT6 acts as an oncogene in this type of tumor. In a first study [9], miRNA miR-34a was shown to counter keratinocyte malignant transformation via a p53/miR-34a/SIRT6 axis, that induces keratinocyte differentiation. In cSCC, loss of p53 or of miR-34a results in SIRT6 overexpression and thereby reduces SCC cell differentiation. SIRT6

silencing in cancerous and healthy keratinocytes, reduces cellular proliferation and is sufficient to trigger a differentiation response similar to the one obtained by miR-34a activation. In a second study [11], Ming and colleagues discovered that SIRT6 regulates COX-2 expression via the AMP-activated protein kinase (AMPK) pathway, affecting inflammation and therefore contributing to skin tumorigenesis. Specifically, following UVB radiation exposure, SIRT6 was shown to become activated by protein kinase B (AKT), and, in turn, to represses AMPK signaling, which upregulates COX-2, known to promote cell proliferation and survival in a cancer niche [22,23]. Moreover, skin-specific SIRT6 deletion in a skin chemical carcinogenesis mouse model, obtained with the 7,12-dimethylbenz[*a*]anthracene (DMBA) – 12-*O*-tetradecanoylphorbol-13-acetate (TPA) protocol, was shown to suppress cell proliferation and epidermal hyperplasia and to consequently reduce tumorigenesis and tumor multiplicity. The key role of SIRT6 in SCC cell proliferation was confirmed by the decreased epidermal hyperplasia following UVR exposure in SIRT6 cKO mice compared to the wild type animals. Taken together, these studies strongly suggest that SIRT6 exerts a pro-oncogenic function in cSCC. Nevertheless, it was also demonstrated that SIRT6 possesses tumor suppressive properties in the same type of tumor [15]. Specifically, such an effect would be achieved through the modulation of aerobic glycolysis (Warburg effect), which was found to be particularly relevant for cSCC cancer stem cells. In this study, again, a DMBA-TPA skin carcinogenesis protocol was utilized and SIRT6 deletion was found to enhance aerobic glycolysis, causing an expansion of the cancer stem cell population. This, in turn, resulted in earlier tumor onset, significantly larger tumors and rapid progression of papillomas into SCCs. In conclusion, SIRT6 appears to also act as a tumor suppressor in cSCC via modulation of glycolysis and by specifically targeting the proliferation of sSCC cancer stem cell.

Given the discrepancy of the studies described above, further work is still needed to clarify the role of SIRT6 in cSCC and whether SIRT6 obstruction or, rather, SIRT6 activation will prove more beneficial for preventing or for treating this condition.

It is widely accepted that pharmacological modulation of the enzymatic activity of sirtuins is a promising strategy to modify disease initiation and/or progression [24]. The SIRT6 inhibitor that has been most studied over the years is compound 2,4-Dioxo-N-(4-(pyridin-3-yloxy)phenyl)−1,2,3,4-tetrahydroquinazoline-6-sulfonamide (PubChem CID:46966788), characterized by a quinazolinedione structure [25], and herewith renamed "S6". It was identified along with other SIRT6 inhibitors in a structure-based screening performed on the CoCoCo database [26] using SIRT6 crystallographic structure [25]. Compound S6 has been tested with success in breast and pancreatic cancer cells (synergic effect with known chemotherapeutics) [27], and for the in vivo treatment of skeletal muscle atrophy [28] and type 2 diabetes [29], and for the prevention of experimental autoimmune encephalomyelitis, an animal model of multiple sclerosis [30]. The best characterized SIRT6 activators, instead, belong to the MDL family of compounds, that feature a N-phenyl-4-(phenylsulfonamido) benzenesulfonamide structure. Compound MDL-800 (PubChem CID:134717374), which was identified through means of Virtual Screening [31], has been exploited in different pathological and physiological processes, such as cancer [31,32], hepatic injuries [33], heart failure associated to diabetes [34], renal inflammation and fibrosis [35].

In this study, we compared the effects of MDL-800 with those of S6 to get further insight on the role of SIRT6 modulation in SCC, using the DMBA-TPA-induced cSCC mouse model.

2. Materials and methods

2.1. Materials

BLD Pharmatech GmbH, Kaiserslautern, Germany provided SIRT6 inhibitor S6 (CAT# BD01051158), as well as the reagents for MDL-800 synthesis, i.e., 5-Bromo-4-fluoro-2-methylaniline (CAT# BD102969);

Methyl 2-(chlorosulfonyl)−5-nitrobenzoate (CAT# BD750937); 3,5-Dichlorobenzene-1-sulfonyl chloride (CAT# BD3150). DMBA (CAT# D3254), TPA (CAT# P8139), IPM, PEG 7 GC, Tween-20, Tween-80, PEG 200 and PEG 400 were obtained from Merck Life Science S.r.l., Milano, Italy. Lipogelag (CAT# 04.3535) and Syntesqual (CAT# 03.1133) were purchased from Vevy Europe S.p.A., Genova, Italy. Solvents used for HPLC analyses and for microemulsion (ME) preparations were of analytical grade.

2.2. MDL-800 chemical synthesis

Compound MDL-800 was synthesized in a 3-step reaction process, adapted from the procedure of Shang et al. [32] and modified as follows. The crude product MDL-800, obtained in the last step, was purified with a preparative HPLC to obtain the final product. The instrument used was Agilent 1260 Infinity preparative HPLC using a column Phenomenex C18 Luna (21.2 × 250 mm, 15 μm). The separation was obtained starting from 30% eluent B and using the following gradient: from 0 to 10 min at 50% eluent B, from 10 min to 35 min at 70% eluent B, from 35 to 45 min at 90% eluent B and from 45 to 60 min at 100% eluent B. Eluent A was water with 0.1% formic acid (FOA) and eluent B was acetonitrile (ACN) with 0.1% FOA. The final product was judged to have a purity of 95% or higher, based on analytical HPLC/MS analysis. Compound purity was determined by integrating peak areas of the chromatogram obtained in liquid phase, monitored at 254 nm.

2.3. Preparation of microemulsions (MEs)

MEs were prepared by adding in a 10 mL corex glass tube 0.4 mL of purified water, 0.1 mL Tween 20, 1.6 mL Syntesqual and 0.4 mL DMSO, containing the compounds S6 or MDL-800. The oil phase was constituted by Syntesqual, whereas the water phase by purified water and Tween 20. Then, the two phases with or without a solution of S6 or MDL-800 in DMSO (blank MEs or MEs containing the compounds), were stirred vigorously with the Ultra-Turrax® T18 Homogenizer (IKA®-Werke GmbH & Co. KG, Germany), which was set at speed 3 (16000 g/min), for 2 min. The concentration of the compounds was 4 mg/mL (9.75 mM) and 10.67 mg/mL (17 mM), for S6 and MDL-800, respectively, so that each dose of 150 μL applied on the dorsal skin (DS) contained 0.6 g (30 mg/kg) of S6 or 1.6 g (80 mg/kg) of MDL-800. Specifically, the choice of these amounts was based on previous animal studies [28–33]: for S6, similar amounts (15–30 mg/kg) were administered intraperitoneally in animal models of Experimental Autoimmune Encephalomyelitis, of Type 2 Diabetes and of muscle atrophy [28–30]; for MDL-800, similar amounts (65–100 mg/kg) were administered intraperitoneally in animal models of hepato-cellular carcinoma and non-small cell lung cancer [31,32].

Since in MEs preparation the scale-up process was not particularly straightforward to achieve, the drug-loaded MEs were carried out repeating multiple times the protocol previously described.

2.4. Physical and chemical stability of microemulsions

Physical stability of the MEs was evaluated after 1, 3 and 7 days from preparation. The formulations were further tested in stability studies: upon storage at 4 °C, they were analyzed at 1, 3 and 6 months. The parameters assessed by visual inspection were fluidity of the mixture, ease of pipetting, phase separation and ability to reach again thermodynamical stability upon shaking.

Chemical stability of the compounds contained in the MEs was also determined. This was accomplished by HPLC analysis. In detail, S6- and MDL-800-loaded MEs were diluted in an acidic/methanol solution (200 mM HCl and 320 mM acetic acid); following centrifugation at 16000 x g for 3 min, the supernatant was injected in HPLC. Analysis was performed in an Agilent Technologies 1260 HPLC, with a ZORBAX® Eclipse Plus C18 3.5 μM, 4.6 mm × 10 mm column, set on 25 °C; injection volume

was 45 μL. The mobile phase consisted of phase A, H_2O + trifluoroacetic acid (TFA) 0.05%, and phase B (ACN + TFA 0.02%); elution was performed with a linear gradient at 1 mL/min. The whole absorbance profile at 220 nm was analyzed.

2.5. Cell culture

SCC13 cell line was obtained from ATCC (LGC Standards S.r.l, Milano, Italy) and cells were maintained in Gibco™ Keratinocyte SFM 1X medium supplied with prequalified human recombinant Epidermal Growth Factor 1–53 (EGF 1–53) and Bovine Pituitary Extract (BPE, CAT# 17005042) (Thermo Fisher Scientific, Milano, Italy), with 50 IU/mL penicillin, and 50 μg/mL streptomycin. Cells were used until passage 5. Cells were cultured in a humidified 5% CO_2 atm at 37 °C. SCC13 cells were treated with compounds S6 or MDL-800 (50 μM), or with vehicle DMSO, as control (maximum DMSO concentration: 0.5%). Proteins were then extracted for Western Blot (WB) analyses (see below), and mRNA for qPCR analyses (see below).

2.6. Animals: cutaneous chemical carcinogenesis and topical treatment with MEs

CD-1 male mice at 56–62 days of age were purchased from Charles River Laboratories Italia S.r.l., Milano, Italy. The generation of D2^{3xflag} has already been described [36]. All animal experiments were carried out in the animal facility of CEINGE-Biotecnologie Avanzate, Napoli, Italy, in accordance with ethical institutional guidelines.

Skin lesions were collected at different time points, following the DMBA-TPA treatment, in which the "initiation" step consists of treatment with a low dose of the mutagen DMBA (100 μL, 1 mg/mL in acetone), and the "promotion" stage consists of treatment with TPA (150 μL, 100 μM in acetone). This procedure induces epidermal proliferation and causes the formation of benign tumors (papillomas) and their progression to invasive SCC. The TPA treatment was continued on the DS until sacrifice. Mice were shaved on their DS prior to DMBA treatment, and later as needed. Any palpable mass greater than 1 mm in size was considered a papilloma and recorded.

CD-1 mice were divided into two groups of approximately 18 mice, and then sub-divided into 3 randomized groups (control, abbreviated in "CTR", S6, MDL-800). Topical application of MEs started in two different stages of skin carcinogenesis. In detail, MEs were applied to the DS of mice (150 μL containing either the vehicle, 0.6 mg S6, or 1.6 mg MDL-800) twice a week with a pipette for viscous liquids, at the promotion stage, together with TPA treatment, or after papillomas arose on the mice skin.

At the termination of the carcinogenesis protocol, after shaving their DS, mice were sacrificed. Immediately, an image of the DS was taken for subsequent, blinded counting of papillomas and evaluation of their size. Tissues were harvested and immediately frozen at −80 °C for further histological, WB and qPCR analyses.

2.7. Western blot analysis

Protein extraction from cells was performed as previously described [37]. Protein extraction from DS and WB analyses were performed as in the work from Nappi et al. [38]. The used primary antibodies and their dilutions are listed in Table 1; loading control was monitored either with anti-Vinculin, anti-Tubulin or anti-H3 specific antibodies.

2.8. mRNA extraction from DS tissues and qPCR

mRNA extraction from cells, retrotranscription and qPCR analyses were performed as previously described [39]. mRNA extraction from DS samples, retrotranscription and qPCR analyses were performed as previously described [38]. Variations to the reported procedure are described here. Retrotranscription was performed with either

Table 1

List of primary antibodies used for western blot (WB) and immunofluorescence (IF) analyses.

Antibody	Supplier	CAT#	Use and dilution
Mouse monoclonal anti-E-cadherin	BD Biosciences	610181	1:500 IF 1:1000 WB
Rabbit monoclonal anti-Vimentin	ABCAM	ab-92547	1:2000 WB 1:1000 IF
Rabbit polyclonal anti-αTubulin	Santa Cruz Biotechnology	SC-5546	1:5000 WB
Rabbit polyclonal anti-cytokeratin 6	COVANCE	PRB-169 P	1:1000 IF
Rat anti-cytokeratin 8	Hybridoma bank	TROMA-I /AB_531826	1:300 IF
Rabbit polyclonal anti-acetylated H3K9	Merck Life Science	H9286	1:10000 WB
Rabbit polyclonal anti-acetylated H3K56	Cell Signalling Technology	4243	1:1000 WB
Rabbit polyclonal anti-histone H3	Cell Signalling Technology	9715	1:5000 WB
Rabbit monoclonal anti-SirT6	Cell Signalling Technology	12486	1:1000 WB
Rabbit polyclonal anti-Keratin 1	Merck Life Science	SAB2101300	1:1000 WB
Rabbit polyclonal anti-Vinculin	Cell Signalling Technology	E1E9V	1:1000 WB
Rabbit polyclonal anti-Glucose Transporter GLUT1	ABCAM	ab-652	1:1000 WB
Mouse monoclonal anti-LDHA	Santa Cruz Biotechnology	SC-130327	1:1000 WB
Rabbit polyclonal anti-PKM	ABCAM	ab-137791	1:1000 WB
Rabbit monoclonal antibody anti-Actin	Cell Signalling Technology	8457	1:1000 WB

Invitrogen™ SuperScript™ VILO™ Master Mix (Life Technologies Italia, Monza, Italy, CAT# 11755–050) or All-In-One 5X RT MasterMix (Microtech Italia S.r.l., Saonara, Italy, CAT# G592). Primer sequences are listed in Table 2.

2.9. Histology and immunostaining of DS tissues

DS from CD-1 mice treated with CTR, S6 and MDL-800 MEs was embedded in paraffin and cut into 7 μm sections; slides were then heated at 37 °C. Sections were stained with Haematoxylin & Eosin (H&E). Alternatively, for staining with immunofluorescence (IF) analyses, slides underwent the procedure previously described [38], with the following variations. The antibodies used are reported in Table 1. Secondary antibodies were anti-rabbit, anti-mouse and anti-rat conjugated to Alexa-Fluor488 or AlexaFluor594 (1:300; Thermo Fisher Scientific).

2.10. Statistical analyses

Statistical analyses were performed with Microsoft Excel, applying Student's two-tailed t test.

3. Results

3.1. SIRT6 pharmacological inhibition induces keratinocyte differentiation in SCC cells

At first, to evaluate if SIRT6 enzymatic activity is affected by the modulators S6 or MDL-800 (Fig. 1A) in an in vitro setting, we used the skin squamous cell carcinoma cell line SCC13 that was treated with either one of the two compounds. The results confirmed that S6 and MDL-800 are effective on keratinocytes: when SIRT6 was inhibited the acetylation level of H3K56, a SIRT6 substrate, increased, whereas it decreased when SIRT6 was activated (Fig. 1B).

As shown in Fig. 1C,D, the pharmacological inhibition of SIRT6 by S6 in SCC13 confirmed the pro-differentiating effects of SIRT6 silencing on cultured keratinocytes [9]. Indeed, S6 enhanced the expression of Keratin 1, 10 and Loricrin, that represent three markers of the cornified layer (Fig. 1C). The increased expression of Keratin 1 was also confirmed by WB analysis (Fig. 1D).
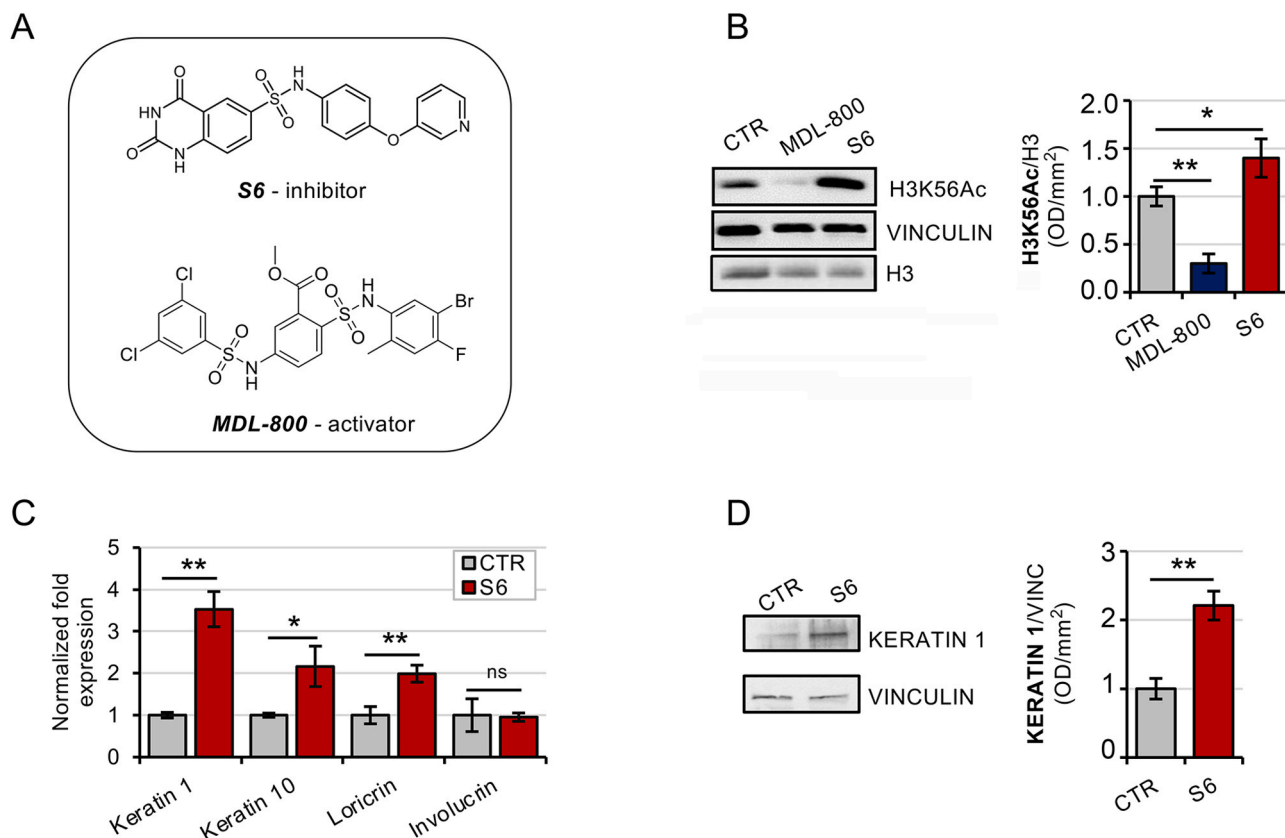
3.2. SIRT6 expression steadily increases at different stages of skin carcinogenesis

Although SIRT6 expression in cSCC has been analyzed by different research groups, that reported its overexpression in cSCC human tissues [10], a profile of SIRT6 levels at different stages of skin carcinogenesis was still unknown. DS samples from DMBA-TPA treated mice [40] were examined: SIRT6 steadily increased during all the stages, from the appearance of papillomas (4 weeks from DMBA treatment), to their conversion into SCCs (30 weeks from DMBA treatment) (Fig. 2).

This result per se suggests that SIRT6 inhibition may represent a promising strategy to treat advanced cSCC. Nevertheless, the administration of either the inhibitor S6 or the activator MDL-800 was planned.

3.3. SIRT6 inhibition in vivo reduces skin carcinogenesis in a preventive approach

After investigating a number of options, including lipogels, oil-in-water (O/W) emulsions and O/W microemulsions (MEs), the chosen formulation to topically administer the SIRT6 modulators was represented by O/W MEs consisting of purified water, Tween 20 as surfactant, the oil Syntesqual and DMSO, which behaved as vehicle for the compounds, with a 4:1 O:W ratio. The formulation was chosen based on the

Table 2

List of oligonucleotides used for qPCR analyses.

Gene	Forward primer (5' → 3')	Reverse primer (5' → 3')	samples
Cyclophilin A	CGCCACTGTCGCTTTTCG	AACTTTGTCTGCAAACAGCTC	Skin tissues
N-cadherin	ACAGTGGAGCTCTACAAAGG	CTGAGATGGGGTTGATAATG	Skin tissues
E-cadherin	CGTCCTGCCAATCCTGATGA	ACCACTGCCCTCGTAATCGAAC	Skin tissues
Zeb1	GCAGAAAATGAGCAAAACCATGA	TGGGTTCTGTATGCAAAGGTG	Skin tissues
Vimentin	GAACCTCCAGGAGGCCGAGG	CATCTTAACATTGAGCAGATC	Skin tissues
Keratin 6	TCGTGACCCTGAAGAAGGATGTA	CCTTGGCTTGCAGTTCAACTT	Skin tissues
Keratin 1	GAAGGAAGGTGGACTCGCTG	TCTCTGCGTTGGTCCTCTTG	Skin tissues
	GAGGATATAGCCCAGAAGAG	ATCTAAGTCTCTGGATCACAC	SCC13 cells
Involucrin	CAGCCACTGGATCAAGCACT	GCTGTGTCCGGTTCTCCAAT	Skin tissues
	TTACTGTGAGTCTGGTTGAC	TCTTTCATTTGCTCCTGATG	SCC13 cells
Keratin 10	AAGAGCAAGGAACTGACTAC	CGTCTCAATTCAGTAATCTCAG	SCC13 cells
Loricrin	ATGATGCTACCCGAGGTTTG	ACTGGGGTTGGGAGGTAGTT	SCC13 cells
Actin	CGGGAAATCGTGCGTGACATTAAG	TGATCTCCTTCTGCATCCTGTCGG	SCC13 cells
Glut-1	ATCCTGCCCACCACGCTCAC	CACGAAGGCCAGCAGGTTCA	Skin tissues
LdhA	CAACATGGCAGCCTTTTCCT	ACCCACCCATGACAGCTTAA	Skin tissues
Pkm2	CTATCCTCTGGAGGCTGTGC	GTGGGGTCGCTGGTAATG	Skin tissues

Fig. 1. SIRT6 pharmacological inhibition induces keratinocyte differentiation. A, Chemical structures of the SIRT-6 inhibitor S6 and of the SIRT-6 activator MDL-800. B, SCC13 cells were incubated for 21 h in the presence or absence (CTR) of S6 or MDL-800 (50 μM). Cell lysates were used for Western blot analyses and total H3 and acetylated H3K56 were detected by immunoblotting. One representative result and mean±SD of 3 quantifications are shown. C-D, SCC13 cells were incubated for 21 h in the presence or absence (CTR) of S6 (50 μM): qPCR analyses of the indicated genes were performed and expression was normalized on Actin levels (n = 3) (C); Western blot analysis of Keratin 1 and Vinculin was performed (one representative result and mean±SD of 3 quantifications are shown) (D). ns, not statistically significant; * p < 0.05; ** p < 0.01.
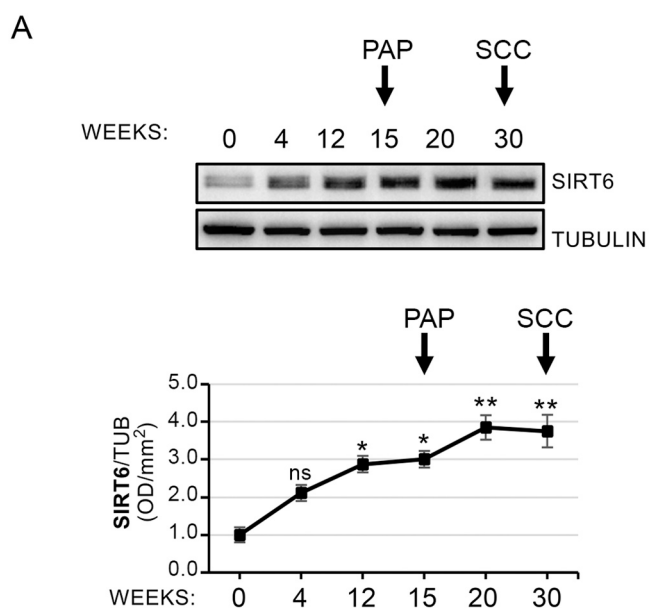
Fig. 2. SIRT6 expression during skin carcinogenesis in a DMBA-TPA mouse model. SIRT6 protein level in DS of mice in healthy skin (0 weeks) and at different stages of skin carcinogenesis of DMBA-TPA treated D2^{3xflag} mice was investigated by Western blot analysis. One representative result and mean±SD of 3 quantifications are shown. ns, not statistically significant; * p < 0.05.

following characteristics: i) high oil:water ratio, since both S6 and MDL-800 are hydrophobic; ii) a balance between the liquid and the semi-solid consistency, easing its administration on the mouse DS; iii) stability of both the modulators and of the formulation for at least a 4 months period (phase did not separate and as the chemical stability of the compounds was confirmed by HPLC/MS); iv) use of excipients approved by official pharmacopeia, particularly suitable for topical administration.

To define the involvement of SIRT6 in the early phases of epidermal tumorigenesis, S6, MDL-800 or their vehicle were applied twice a week at the beginning of the promotion stage of the DMBA-TPA-induced carcinogenesis, simultaneously to the first TPA application, in CD-1 mice (Fig. 3A).

SIRT6 modulation by S6 and MDL-800 was assessed by evaluating the acetylation levels of H3K56, the most specific SIRT6 substrate, by WB analyses: when SIRT6 was inhibited by S6, H3K56 acetylation level increased, whereas when activated by MDL-800, H3K56 acetylation level decreased, compared to control group (Fig. 3B). This result confirmed that the microemulsions were able to pass the skin barrier, effectively releasing the compounds to the epidermis, where they reached their target. As shown in Fig. 1S, the expression levels of GLUT-1, LDHA and PKM2 further demonstrated that the administration of S6 and MDL-800 was able to modulate SIRT6 activity [25,29].

Tumor incidence was evaluated by visual inspection at 13 weeks (intermediate time point) and at 17 weeks (sacrifice) from the DMBA application (Fig. 3A). S6 administration exerted an anti-proliferative effect on the skin lesions, as they were significantly less in frequency than in the control group, at both timepoints (Fig. 3C,D). Moreover, S6
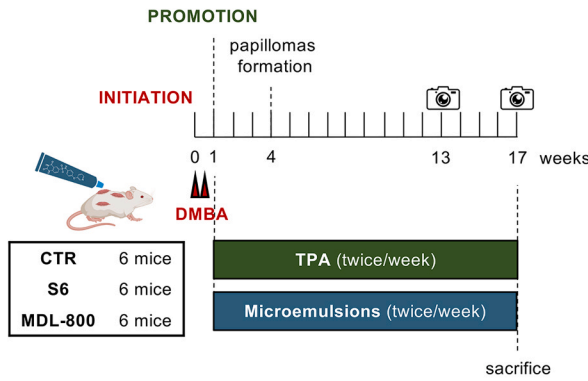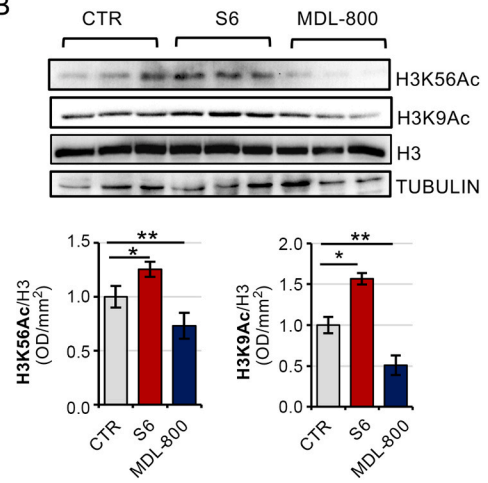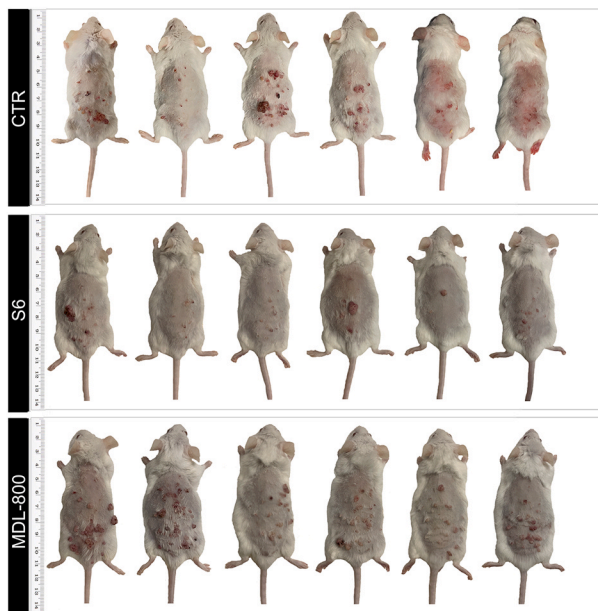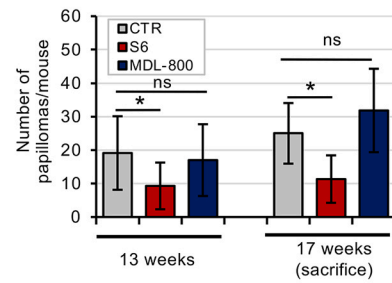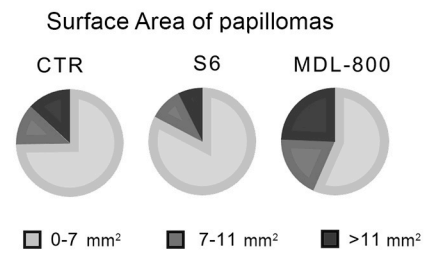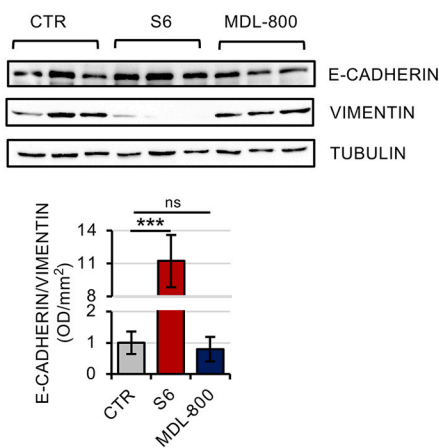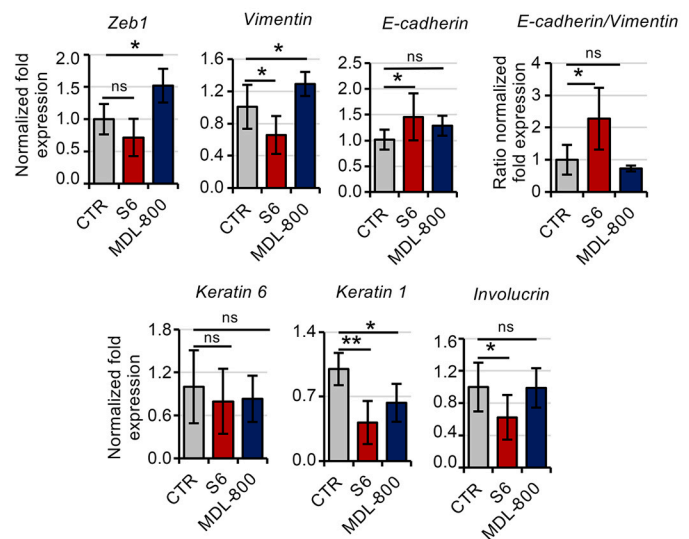
(caption on next page)

Fig. 3. SIRT6 inhibition delays skin carcinogenesis in a preventive approach: papilloma quantification, Western blot analysis and qPCR. A, Treatment plan, in a preventive approach, of the DS of the 2-stage carcinogenesis mouse model with MEs containing either the SIRT-6 activator MDL-800, the SIRT-6 inhibitor S6 or the vehicle DMSO (CTR): MEs were applied as the promotion stage with TPA was started (n = 6 mice/group). B, Western blot analyses were performed on DS lysates to evaluate the acetylation levels of H3K9 and H3K56. C, Appearance of the DS of mice treated with the SIRT-6 modulators in a preventive approach, at sacrifice (17 weeks). D, Frequency of papillomas on the DS of the mice at an intermediate timepoint (13 weeks) and at sacrifice (17 weeks). E, Area distribution of papillomas on the DS of the mice at sacrifice (17 weeks). F, Western blot analyses were performed on DS lysates to evaluate the levels of the EMT markers E-cadherin and Vimentin. G, qPCR analyses to evaluate the expression of: markers indicating EMT progression (Zeb1, E-cadherin and Vimentin), and the ratio E-cadherin/Vimentin; the epidermal hyper-proliferation marker Keratin 6; the keratinocyte differentiation markers Keratin 1 and Involucrin. ns, not statistically significant; * p < 0.05; ** p < 0.01; *** p < 0.001.

increased the percentage of lesions smaller than 7 mm^2 and decreased the number of large lesions (with an area bigger than 11 mm^2), compared to control mice (Fig. 3C,E).

Conversely, MDL-800-treated mice developed approximately a number of papillomas comparable to the control group (Fig. 3C,D). However, the lesions were significantly larger in MDL-800-treated mice, hinting an involvement of SIRT6 in the skin proliferation processes.

Next, the effect of SIRT6 pharmacological modulation on epithelial-
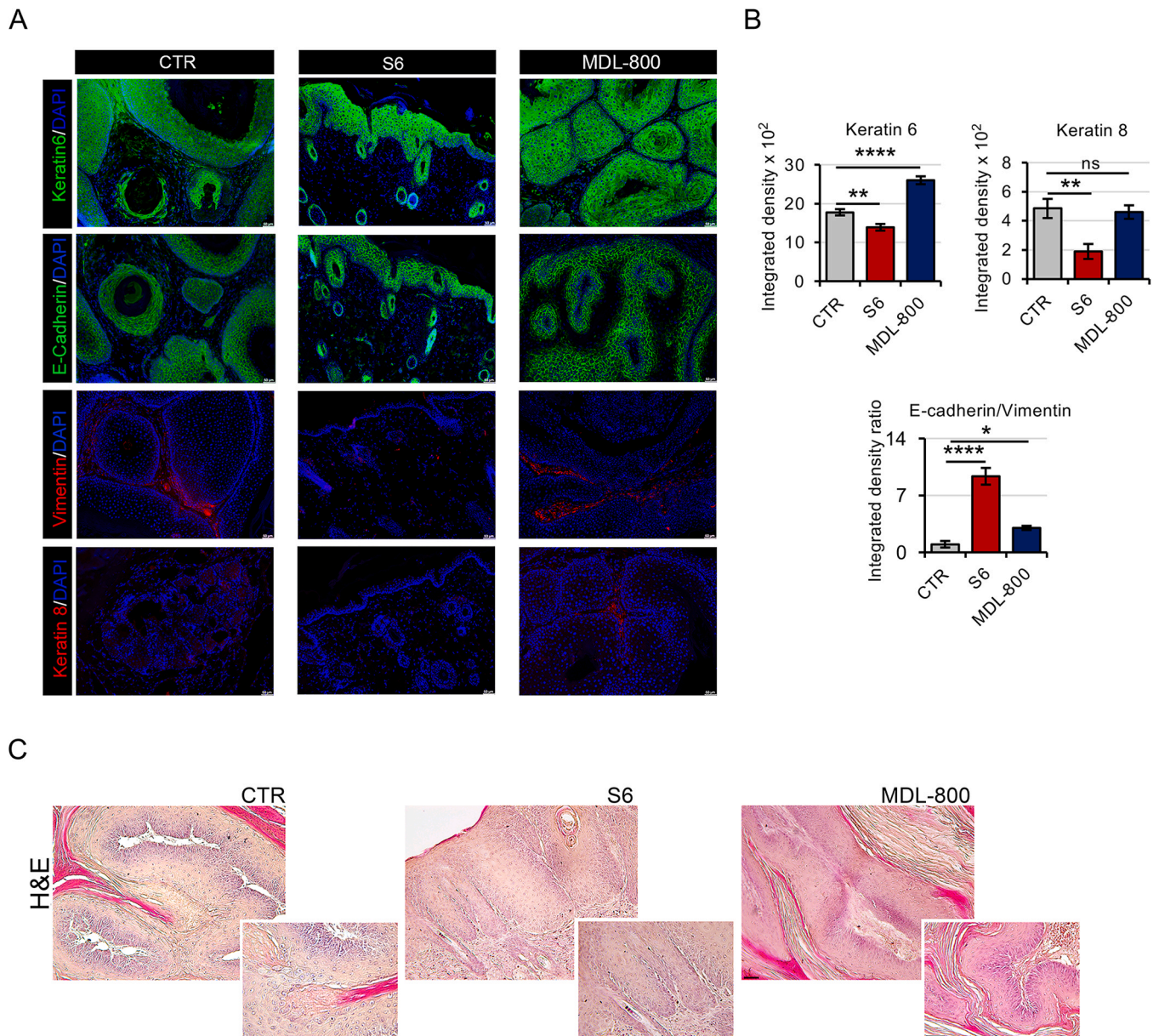
Fig. 4. SIRT6 inhibition delays skin carcinogenesis in a preventive approach: histology and immunofluorescence. Skin cancer was induced in mice following the DMBA-TPA protocol, as described in Materials and Methods. Administration of vehicle (CTR), S6 or MDL-800 started at day 7 from the first DMBA application (see scheme in Fig. 3A; n = 6 mice/group). A, Immunofluorescence staining for: the EMT markers E-cadherin and Vimentin, the epidermal hyperproliferating marker Keratin 6, the skin tumor marker Keratin 8. Bar: 50 μm. 10x magnification. Representative images are shown. B, Densitometric analysis of the levels of Keratin 6 and Keratin 8, and the ratio of E-cadherin/Vimentin of the immunofluorescence staining (mean±SD of n = 3 quantifications). C, Haematoxylin & Eosin staining of histological sections of DS samples Bar: 50 μm. 10x and 20x magnifications. Representative images are shown. ns, not statistically significant; * p < 0.05; ** p < 0.01; **** p < 0.0001.

to-mesenchymal transition (EMT) was investigated, since EMT is critically involved in the progression of epithelial tumor toward invasiveness. The expression level of E-cadherin and Vimentin, and their ratio (used as an indicator of EMT progression), indicated that SIRT6 inhibition by S6 decreased the EMT process: indeed, WB, qPCR and IF analyses demonstrated that Vimentin is less abundant in S6-treated lesions (Figs. 3F,G and 4A); conversely, E-cadherin was more expressed when SIRT6 was inhibited, as demonstrated by qPCR and IF analyses (Figs. 3G and 4A). Zeb1 expression showed a trend to be decreased in S6-treated papillomas, although statistical significance was not reached, whereas it was significantly increased by SIRT6 activation by MDL-800 (Fig. 3G), in comparison to control conditions. In addition, MDL-800 did not significantly affect the E-cadherin/Vimentin ratio. Keratin 1 and Involucrin, which are usually more expressed at the papilloma level compared to healthy skin [41], were significantly reduced by S6, as detected by qPCR (Fig. 3G).

IF analysis indicated that Keratin 6, which is often upregulated in hyperproliferative stages of epidermis [42], is reduced by S6 and enhanced by MDL-800, confirming that SIRT6 modulation affects keratinocytes proliferation during the chemically induced carcinogenesis (Fig. 4A,B). In agreement with the mRNA profile of E-cadherin and of Vimentin shown in Fig. 3G, IF analysis demonstrated that S6 increases the E-cadherin/Vimentin ratio (Fig. 4A,B). Lastly, Keratin 8, a typical marker of advanced SCC epidermis [42], was significantly reduced by S6 (Fig. 4A,B) when compared to control mice.

Also the histological examination of papillomas by H&E confirmed the more advanced stage of tumor progression in MDL-800-treated papillomas compared to the control group, whereas lesions of S6-treated mice morphologically appeared as more similar to still structured skin (Fig. 4C).

Together, these data suggest that SIRT6 is essential for the shift from a papilloma stage to a more advanced stage of SCC: indeed, during its inhibition, the epithelial phenotype is maintained and delays further progression.

3.4. SIRT6 inhibition in vivo delays skin carcinogenesis in a therapeutic approach

To define the effect of the modulation of the enzymatic activity of SIRT6 in a therapeutic approach, S6, MDL-800 or their vehicle were administered 5 weeks after papilloma formation in CD-1 mice (Fig. 5A).

Tumor incidence was evaluated by visual inspection at 13 weeks (i. e., after 4 weeks of treatment; intermediate time point) and at 28 weeks (sacrifice) (Fig. 5B-D). Treatments were performed for 3 months, and then suspended to evaluate whether the compounds' effects were maintained (Fig. 5A).

Visual inspection of mice DS at 13 and 28 weeks, showed that S6 reduced papillomas' frequency at the intermediate timepoint compared to control group, whereas at sacrifice this trend was lost (Fig. 5B,C). MDL-800, instead, had no effect at the intermediate timepoint on the overall number of papillomas compared to the control group, while at sacrifice SIRT6 activation dramatically increased it (Fig. 5B,C). Regarding the size, papillomas with area > 30 mm^2 were less frequent in S6-treated than in control mice (Fig. 5B,D). Conversely, MDL-800 treatment determined an increased number of papillomas and a higher percentage of lesions with area > 30 mm^2, compared to the control group (Fig. 5B,D).

Gene expression analyses demonstrated that mRNA levels of the markers of EMT N-cadherin, Zeb1 and Vimentin are less enhanced in S6-treated animals than in control mice (Fig. 5E), indicating a less advanced EMT at the time of sacrifice. Although E-cadherin was not significantly modified, the ratio E-cadherin/Vimentin was significantly higher in the S6 group (Fig. 5E), as also confirmed by IF results (Fig. 6A,C). Also the epidermal hyperproliferation appeared to be reduced in S6-treated lesions, since Keratin 6 expression was significantly lower than the vehicle-treated ones, as indicated by qPCR (Fig. 5E) and IF (Fig. 6A,C)

analyses. Finally, the cSCC tumor marker Keratin 8 was expressed at lower levels in S6-treated mice (Fig. 6A,B).

MDL-800 did not significantly modify the expression of any of the examined genes (Fig. 5E). In IF analysis, MDL-800 appeared to increase the expression of Keratin 6 (Fig. 6A,B), in line with larger and more numerous papillomas in this treatment group. The histological examination by H&E confirmed that, at the time of sacrifice, skin lesions were papillomas in all the three treatment groups, not yet converted to SCCs (Fig. 6C).

Taken together, these findings reveal a crucial role of SIRT6 in regulating SCC tumor progression and suggest that targeting SIRT6 may represent a general tool to reduce the EMT and the invasiveness of skin carcinogenesis.

4. Discussion

This represents the first study in which SIRT6 is pharmacologically targeted in cSCC. Until now, research to investigate the role of SIRT6 in this type of cancer had been performed solely on SIRT6 KO mice or on SIRT6 silenced SCC cells. Pharmacological modulation of an enzyme, compared to its genetic modification, however, represents an approach more similar to current cancer treatment strategies.

In fact, this study represents the first pharmacological modulation of any sirtuin isoform in this cancer type. Research on sirtuins and cSCC has been done so far on SIRT1 and −6, and to a minor extent on SIRT2. SIRT1 can be identified as a tumor promoter in cSCC, with studies showing its involvement in two pathways that are implicated in cSCC development: i) the modulation of the miR-199a-5p/SIRT1/CD44ICD axis results in the repression of cSCC stem cells, and therefore also of tumor formation and migration [12]; ii) the miR-30c/SIRT1 axis, according to which miRNA MiR-30c overexpression in SCC cells downregulates SIRT1, thereby suppressing cell proliferation and chemotherapeutic resistance [13]. SIRT2, similarly to the other sirtuins, is overexpressed in cSCC both at the mRNA and at the protein levels [10]. A separate study, though, has shown that SIRT2 protein is downregulated in cSCC and that SIRT2 KO increases tumor growth in a DMBA-TPA skin cancer mouse model, suggesting that SIRT2 has pro-differentiating and oncosuppressive roles in cSCC [14]. Given the discrepancy between different studies, further elucidation of SIRT2 function in cSCC is still necessary. Based on the literature, also SIRT6 has been reported with either a tumor promoter or suppressive function (see Introduction). Therefore, our aim was to evaluate the effects of both SIRT6 pharmacological inhibition and activation, to compare both types of modulation in cSCC. The pharmacological modulation of SIRT6 in cSCC was evaluated in vivo in a two-stage skin carcinogenesis mouse model, namely the one obtained from the DMBA-TPA 2-stage carcinogenesis protocol. The formulation type chosen for their topical treatment was the O/W microemulsion technology, which allows the dissolution of both compounds, that are quite lipophilic, and facilitate drug absorption after topical application. The formulations prepared were specifically O/W MEs. Admittedly, although the DMBA-TPA 2-stage carcinogenesis mouse model can be considered one of the most suitable to study cSCC for its high reproducibility, it presents some limitations: i) the absence of correspondence of mice papillomas to any human skin cancer condition, even though the late SCCs from this mouse model are a good representation of human ones; ii) the lack of full correlation of the genes involved in the first stages of tumorigenesis between human NMSC and the initiation process in the DMBA-TPA mouse model, since mutations in p53 are more relevant for human cSCC, while Hras is crucial in murine carcinogenesis [43]; iii) the rate of metastasis of skin tumors in the mouse model is quite low, making this protocol of limited utility to study metastasis [44].

Nevertheless, as mentioned above, this model is widely used. Our results suggest that SIRT6 pharmacological inhibition is beneficial in delaying skin carcinogenesis, specifically by reducing keratinocyte hyperproliferation and by determining a less advanced EMT program. A
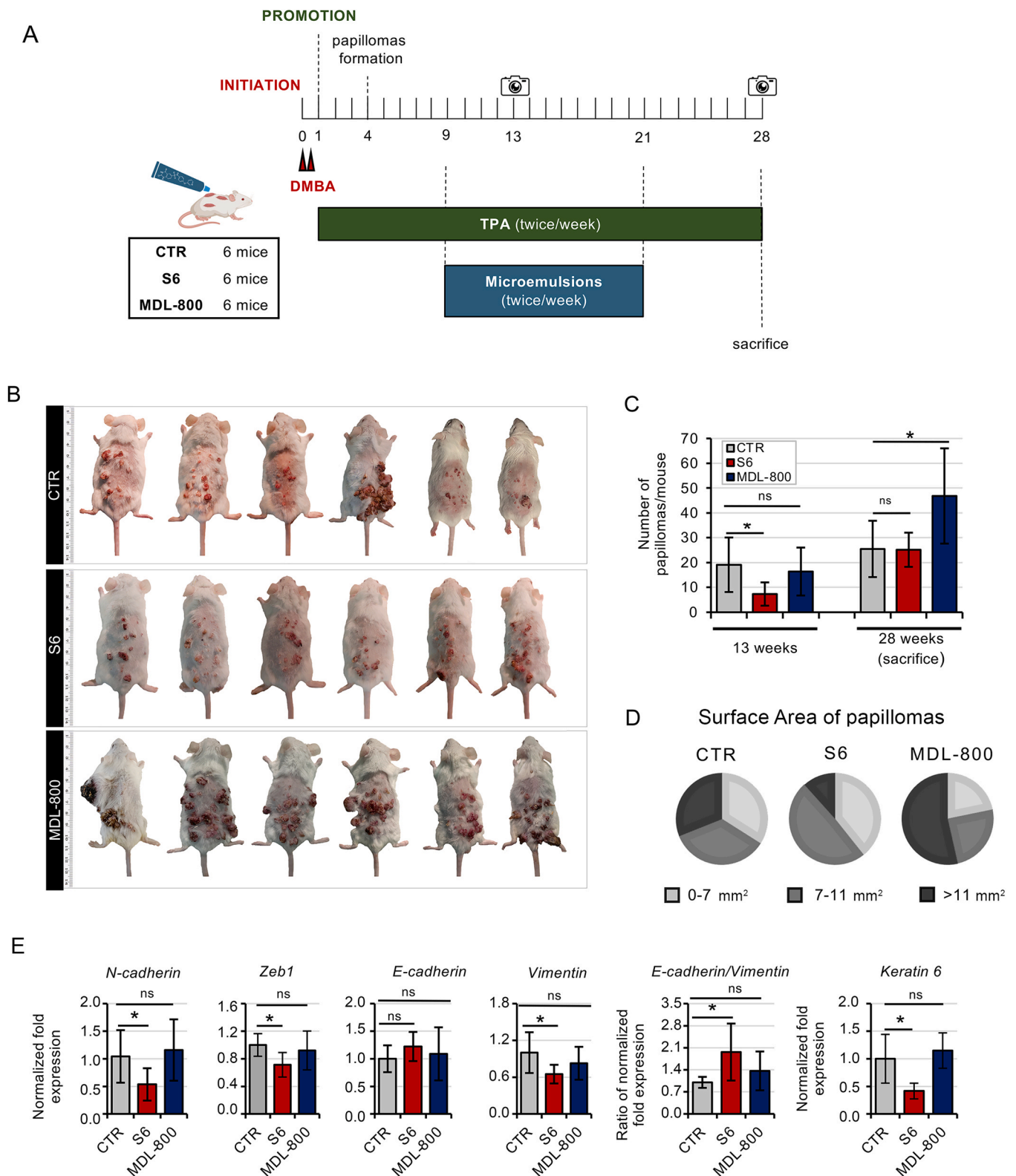
Fig. 5. SIRT6 inhibition attenuates skin carcinogenesis in a therapeutic approach: papilloma quantification, Western blot analysis and qPCR. A, Treatment plan, in a therapeutic approach, of the DS of the 2-stage carcinogenesis mouse model with MEs containing either the SIRT6 activator MDL-800, the SIRT6 inhibitor S6 or the vehicle DMSO (CTR): treatment with MEs was administered after 5 weeks of the appearance of the papillomas on the DS of all mice (n = 6 mice/group). B, Appearance of the DS of mice treated with the SIRT6 modulators in a preventive approach, at sacrifice (28 weeks). C, Frequency of papillomas on the DS of the mice at an intermediate timepoint (13 weeks) and at sacrifice (28 weeks). D, Area distribution of papillomas on the DS of the mice at sacrifice (28 weeks). E, qPCR analysis to evaluate the expression of: markers indicating EMT progression (N-cadherin, Zeb1, E-cadherin and Vimentin), and the ratio E-cadherin/Vimentin; the epidermal hyper-proliferation marker Keratin 6. ns, not statistically significant; * p < 0.05.
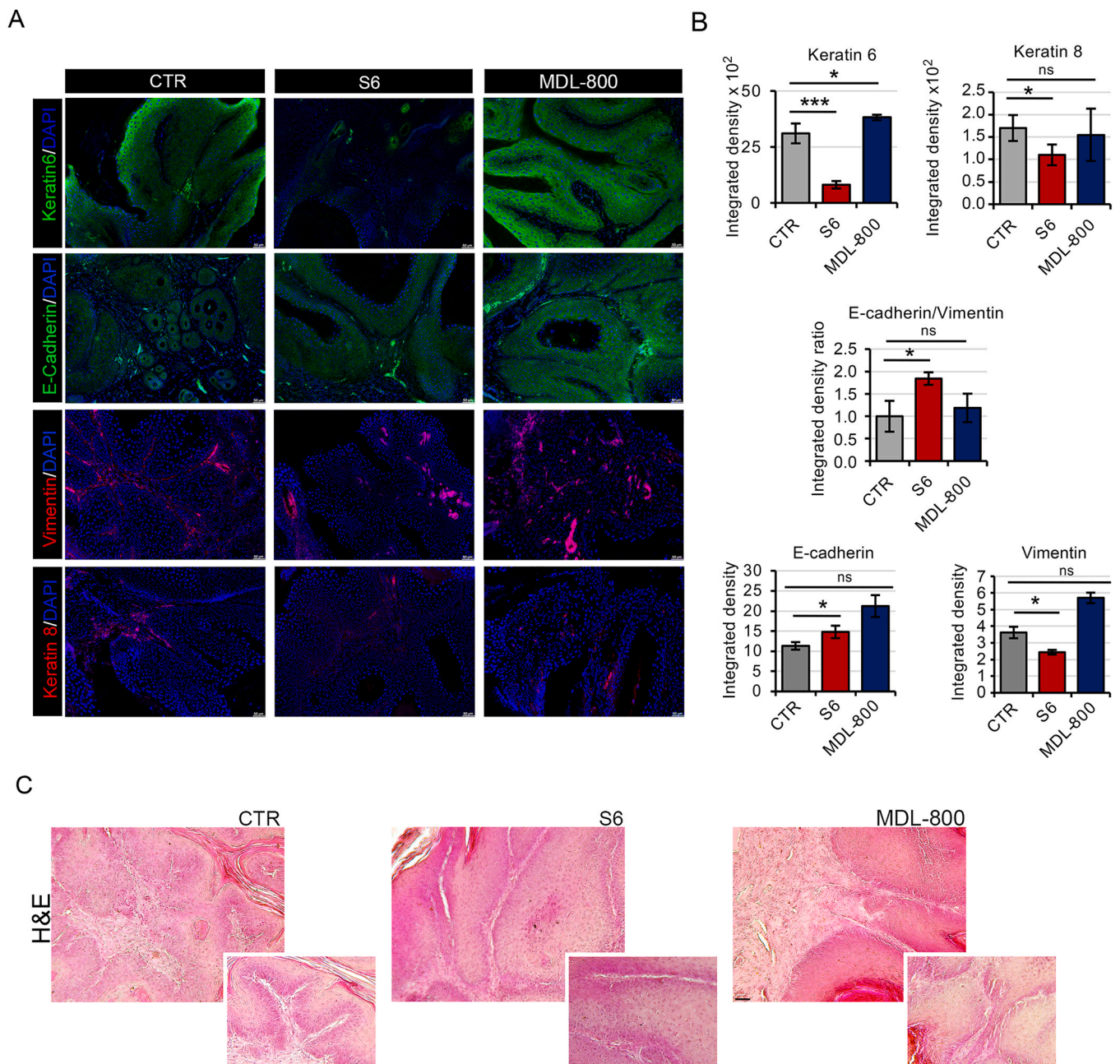
Fig. 6. SIRT6 inhibition attenuates skin carcinogenesis in a therapeutic approach: histology and immunofluorescence. Skin cancer was induced in mice following the DMBA-TPA protocol, as described in Materials and Methods. Administration of vehicle (CTR), S6 or MDL-800 started at day 50 from the first DMBA application (see scheme in Fig. 5A; n = 6 mice/group). A, Immunofluorescence staining for: the EMT markers E-cadherin and Vimentin, the epidermal hyperproliferating marker Keratin 6, the skin tumor marker Keratin 8. Bar: 50 μm. Representative images are shown. B, Densitometric analysis of the levels of Keratin 6 and Keratin 8, and the ratio of E-cadherin/Vimentin of the immunofluorescence staining (mean±SD of n = 3 quantifications). C, Haematoxylin & Eosin staining of histological sections of DS samples Bar: 50 μm. 10x and 20x magnification. Representative images are shown. ns, not statistically significant; * $p < 0.05$; *** $p < 0.001$.

number of possible mechanisms may underlie a less advanced EMT and carcinogenesis by inhibiting SIRT6. SIRT6 has been reported to display an oncogenic activity through different pathways, such as the SIRT6/Snail/KLF4 axis [45,46], the Wnt/β-catenin signaling one [47,48], or the COX-2/AMPK one [11]. More specifically, SIRT6 inhibition may have increased the expression of the tumor suppressor Kruppel-like factor 4 (KLF4), thus resulting in an anti-cancer effect, as reported in non-small cell lung cancer (NSCLC) cells [45]. Moreover, the tumor suppressive properties of KFL4 in SCCs have been demonstrated: in cancerous keratinocytes SCC12 and SCC13, KLF4 overexpression decreased cell proliferation, reduced the cellular invasive potential, and the EMT-related Vimentin [46]. Alternatively, SIRT6 inhibition may

have interfered with the Wnt/β-catenin signaling, a well-known pathway associated with the functional regulation of multiple cancer types, suppressing proliferation and EMT [49]. Zhang and coll. observed that SIRT6 silencing suppressed the proliferation and metastasis of prostate cancer in vitro, by reducing the levels of β-catenin, Cyclin D1 and c-myc [47]. Accordingly, Jang and coll. reported that SIRT6 silencing activated β-catenin and reduced the abundancy of EMT-related molecules, such as Snail, Vimentin and N-cadherin, resulting in attenuated EMT in ovarian cancer cells [48]. Finally, a possible mechanism explaining the anti-cancer effect of SIRT6 inhibition in our study, is represented by the downregulation of the pro-inflammatory and pro-survival protein COX-2. Indeed, Ming and coll. demonstrated that in

skin specific SIRT6 cKO mice undergoing a DMBA-TPA protocol, SIRT6 deletion inhibited tumorigenesis, by suppressing epidermal proliferation and hyperplasia, since SIRT6 regulates COX-2 stability through blockade of the AMPK pathway [11].

5. Conclusion

Two protocols were followed for the application of the SIRT6 modulators on the DS of mice. The first one consisted in performing the treatment at the beginning of the promotion stage of the DMBA-TPA protocol (preventive approach). In the second one, the application of the SIRT6 modulators on the DS of mice was started several weeks after the first appearance of the papillomas (therapeutic approach). Given the encouraging results obtained with the SIRT6 inhibitor delaying skin carcinogenesis in a preventive approach and given the promising appearance of the DS of mice during the cancer treatment, when treating mice in the therapeutic approach, we decided to interrupt the application of the modulators (Fig. 5A), to evaluate if the beneficial effect of the SIRT6 inhibitor was maintained. Indeed, a less advanced carcinogenesis was retained throughout the following period without treatment, as mice of the SIRT6 inhibitor group presented less advanced EMT (Figs. 5, 6).

As for SIRT6 activation, we did not observe it leading to an opposite effect to SIRT6 inhibition. A possible explanation may be found in the null effect of activating an enzyme that is already overexpressed in the carcinogenic stages (Fig. 2), therefore without presenting an additive effect. On the other hand, the fact that MDL-800 failed to decrease carcinogenesis may not necessarily be in contrast with previous results demonstrating the oncosuppressive role of SIRT6 [15]: in our study, the progression of the carcinogenic process was evaluated by analyzing the bulk tumor masses and not the abundancy of the CSC population.

In conclusion, SIRT6 inhibition delays skin cancer progression. An optimized time window for the treatment would need to be carefully defined for translation of SIRT6 targeting into the clinical setting.

CRediT authorship contribution statement

A.Nencioni, and **S.B**: Conceptualization; **E.A.**, **C.M.**, **F.P.**, **A.S.**, **M.M.** and **A. Nappi**, Visualization, Investigation; **E.R.**, **E.C.**, and **A.D.R.**: Methodology; **E.A.** and **C.M.**: Data curation; **E.R.**, **E.M.**, **L.S.**, **A.Nencioni**, **S.B**: Supervision; **E.A.** and **S.B.**: Writing – original draft preparation; **C.M.**, **F.P.**, **A.D.F.**, and **S.B.**: Writing and Editing; **A.Nencioni** and **S.B.**: Funding acquisition.

Declaration of Competing Interest

The authors declare that they have no known competing financial interests or personal relationships that could have appeared to influence the work reported in this paper.

Appendix A. Supporting information

Supplementary data associated with this article can be found in the online version at doi:10.1016/j.biopha.2023.115326.

References

[1] R. Gordon, Skin cancer: an overview of epidemiology and risk factors, Semin Oncol. Nurs. 29 (3) (2013) 160–169.

[2] A.J. Stratigos, C. Garbe, C. Dessinioti, C. Lebbe, V. Bataille, L. Bastholt, et al., European interdisciplinary guideline on invasive squamous cell carcinoma of the skin: Part 2. treatment, Eur. J. Cancer 128 (2020) 83–102.

[3] P. Nagarajan, M.M. Asgari, A.C. Green, S.M. Guhan, S.T. Arron, C.M. Proby, et al., Keratinocyte Carcinomas: current concepts and future research priorities, Clin. Cancer Res. 25 (8) (2019) 2379–2391.

[4] A. Chalkiadaki, L. Guarente, The multifaceted functions of sirtuins in cancer, Nat. Rev. Cancer 15 (10) (2015) 608–624.

[5] E. Abbotto, N. Scarano, F. Piacente, E. Millo, E. Cichero, S. Bruzzone, Virtual screening in the identification of sirtuins' activity modulators, Molecules 27 (17) (2022) 5641.

[6] Q.J. Wu, T.N. Zhang, H.H. Chen, X.F. Yu, J.L. Lv, Y.Y. Liu, et al., The sirtuin family in health and disease, Signal Transduct. Target Ther. 7 (1) (2022), 402.

[7] L. Bosch-Presegue, A. Vaquero, The dual role of sirtuins in cancer, Genes Cancer 2 (6) (2011) 648–662.

[8] L.M. Garcia-Peterson, M.J. Wilking-Busch, M.A. Ndiaye, C.G.A. Philippe, V. Setaluri, N. Ahmad, Sirtuins in skin and skin cancers, Ski. Pharmacol. Physiol. 30 (4) (2017) 216–224.

[9] K. Lefort, Y. Brooks, P. Ostano, M. Cario-Andre, V. Calpini, J. Guinea-Viniegra, et al., A miR-34a-SIRT6 axis in the squamous cell differentiation network, EMBO J. 32 (16) (2013) 2248–2263.

[10] C.A. Benavente, S.A. Schnell, E.L. Jacobson, Effects of niacin restriction on sirtuin and PARP responses to photodamage in human skin, PloS One 7 (7) (2012), e42276.

[11] M. Ming, W. Han, B. Zhao, N.R. Sundaresan, C.X. Deng, M.P. Gupta, et al., SIRT6 promotes COX-2 expression and acts as an oncogene in skin cancer, Cancer Res. 74 (20) (2014) 5925–5933.

[12] R.H. Lu, Z.Q. Xiao, J.D. Zhou, C.Q. Yin, Z.Z. Chen, F.J. Tang, et al., MiR-199a-5p represses the stemness of cutaneous squamous cell carcinoma stem cells by targeting Sirt1 and CD44ICD cleavage signaling, Cell Cycle 19 (1) (2020) 1–14.

[13] T. Liu, F. Jiang, L.Y. Yu, Y.Y. Wu, Lidocaine represses proliferation and cisplatin resistance in cutaneous squamous cell carcinoma via miR-30c/SIRT1 regulation, Bioengineered 13 (3) (2022) 6359–6370.

[14] M. Ming, L. Qiang, B. Zhao, Y.Y. He, Mammalian SIRT2 inhibits keratin 19 expression and is a tumor suppressor in skin, Exp. Dermatol. 23 (3) (2014) 207–209.

[15] J.E. Choi, C. Sebastian, C.M. Ferrer, C.A. Lewis, M. Sade-Feldman, T. LaSalle, et al., A unique subset of glycolytic tumor-propagating cells drives squamous cell carcinoma, Nat. Metab. 3 (2) (2021) 182–195.

[16] R.I. Khan, S.S.R. Nirzhor, R. Akter, A review of the recent advances made with SIRT6 and its implications on aging related processes, major human diseases, and possible therapeutic targets, Biomolecules 8 (3) (2018).

[17] C. Sebastian, F.K. Satterstrom, M.C. Haigis, R. Mostoslavsky, From sirtuin biology to human diseases: an update, J. Biol. Chem. 287 (51) (2012) 42444–42452.

[18] G. Liu, H. Chen, H. Liu, W. Zhang, J. Zhou, Emerging roles of SIRT6 in human diseases and its modulators, Med Res. Rev. 41 (2) (2021) 1089–1137.

[19] L. Zhong, A. D'Urso, D. Toiber, C. Sebastian, R.E. Henry, D.D. Vadysirisack, et al., The histone deacetylase Sirt6 regulates glucose homeostasis via Hif1alpha, Cell 140 (2) (2010) 280–293.

[20] J.E., Jr Dominy, Y. Lee, M.P. Jedrychowski, H. Chim, M.J. Jurczak, J.P. Camporez, et al., The deacetylase Sirt6 activates the acetyltransferase GCN5 and suppresses hepatic gluconeogenesis, Mol. Cell 48 (6) (2012) 900–913.

[21] S. Elhanati, Y. Kanfi, A. Varvak, A. Roichman, I. Carmel-Gross, S. Barth, et al., Multiple regulatory layers of SREBP1/2 by SIRT6, Cell Rep. 4 (5) (2013) 905–912.

[22] K.S. Chun, J.K. Akunda, R. Langenbach, Cyclooxygenase-2 inhibits UVB-induced apoptosis in mouse skin by activating the prostaglandin E2 receptors, EP2 and EP4, Cancer Res. 67 (5) (2007) 2015–2021.

[23] S.M. Fischer, A. Pavone, C. Mikulec, R. Langenbach, J.E. Rundhaug, Cyclooxygenase-2 expression is critical for chronic UV-induced murine skin carcinogenesis, Mol. Carcinog. 46 (5) (2007) 363–371.

[24] F. Fiorentino, A. Mai, D. Rotili, Emerging therapeutic potential of SIRT6 modulators, J. Med. Chem. 64 (14) (2021) 9732–9758.

[25] M.D. Parenti, A. Grozio, I. Bauer, L. Galeno, P. Damonte, E. Millo, et al., Discovery of novel and selective SIRT6 inhibitors, J. Med. Chem. 57 (11) (2014) 4796–4804.

[26] A. Del Rio, A.J. Barbosa, F. Caporuscio, G.F. Mangiatordi, CoCoCo: a free suite of multiconformational chemical databases for high-throughput virtual screening purposes, Mol. BioSyst. 6 (11) (2010) 2122–2128.

[27] G. Sociali, L. Galeno, M.D. Parenti, A. Grozio, I. Bauer, M. Passalacqua, et al., Quinazolinedione SIRT6 inhibitors sensitize cancer cells to chemotherapeutics, Eur. J. Med. Chem. 102 (2015) 530–539.

[28] S. Mishra, C. Cosentino, A.K. Tamta, D. Khan, S. Srinivasan, V. Ravi, et al., Sirtuin 6 inhibition protects against glucocorticoid-induced skeletal muscle atrophy by regulating IGF/PI3K/AKT signaling, Nat. Commun. 13 (1) (2022), 5415.

[29] G. Sociali, M. Magnone, S. Ravera, P. Damonte, T. Vigliarolo, M. Von Holtey, et al., Pharmacological Sirt6 inhibition improves glucose tolerance in a type 2 diabetes mouse model, FASEB J. 31 (7) (2017) 3138–3149.

[30] G. Ferrara, A. Benzi, L. Sturla, D. Marubbi, D. Frumento, S. Spinelli, et al., Sirt6 inhibition delays the onset of experimental autoimmune encephalomyelitis by reducing dendritic cell migration, J. Neuroinflamm. 17 (1) (2020), 228.

[31] Z. Huang, J. Zhao, W. Deng, Y. Chen, J. Shang, K. Song, et al., Identification of a cellularly active SIRT6 allosteric activator, Nat. Chem. Biol. 14 (12) (2018) 1118–1126.

[32] J.L. Shang, S.B. Ning, Y.Y. Chen, T.X. Chen, J. Zhang, MDL-800, an allosteric activator of SIRT6, suppresses proliferation and enhances EGFR-TKIs therapy in non-small cell lung cancer, Acta Pharmacol. Sin. 42 (1) (2021) 120–131.

[33] J. Zhang, Y. Li, Q. Liu, Y. Huang, R. Li, T. Wu, et al., Sirt6 alleviated liver fibrosis by deacetylating conserved lysine 54 on Smad2 in hepatic stellate cells, Hepatology 73 (3) (2021) 1140–1157.

[34] X. Wu, H. Liu, A. Brooks, S. Xu, J. Luo, R. Steiner, et al., SIRT6 mitigates heart failure with preserved ejection fraction in diabetes, Circ. Res. 131 (11) (2022) 926–943.

[35] J. Jin, W. Li, T. Wang, B.H. Park, S.K. Park, K.P. Kang, Loss of proximal tubular sirtuin 6 aggravates unilateral ureteral obstruction-induced tubulointerstitial inflammation and fibrosis by regulation of beta-catenin acetylation, Cells 11 (9) (2022).

[36] M.G. Castagna, M. Dentice, S. Cantara, R. Ambrosio, F. Maino, T. Porcelli, et al., DIO2 Thr92Ala reduces deiodinase-2 activity and Serum-T3 levels in thyroid-deficient patients, J. Clin. Endocrinol. Metab. 102 (5) (2017) 1623–1630.

[37] C. Astigiano, F. Piacente, M.E. Laugieri, A. Benzi, C.A. Di Buduo, C.P. Miguel, et al., Sirtuin 6 regulates the activation of the ATP/Purinergic Axis in Endothelial Cells, Int. J. Mol. Sci. 24 (7) (2023) 6759.

[38] A. Nappi, C. Miro, A. Pezone, A. Tramontano, E. Di Cicco, S. Sagliocchi, et al., Loss of p53 activates thyroid hormone via type 2 deiodinase and enhances DNA damage, Nat. Commun. 14 (1) (2023) 1244–1261.

[39] P. Becherini, I. Caffa, F. Piacente, P. Damonte, V.G. Vellone, M. Passalacqua, et al., SIRT6 enhances oxidative phosphorylation in breast cancer and promotes mammary tumorigenesis in mice, Cancer Metab. 9 (1) (2021), 6.

[40] C. Miro, E. Di Cicco, R. Ambrosio, G. Mancino, D. Di Girolamo, A.G. Cicatiello, et al., Thyroid hormone induces progression and invasiveness of squamous cell carcinomas by promoting a ZEB-1/E-cadherin switch, Nat. Commun. 10 (1) (2019), 5410.

[41] E.L. Abel, J.M. Angel, K. Kiguchi, J. DiGiovanni, Multi-stage chemical carcinogenesis in mouse skin: fundamentals and applications, Nat. Protoc. 4 (9) (2009) 1350–1362.

[42] R. Moll, M. Divo, L. Langbein, The human keratins: biology and pathology, Histochem Cell Biol. 129 (6) (2008), 705-33.

[43] C.L. Benjamin, H.N. Ananthaswamy, p53 and the pathogenesis of skin cancer, Toxicol. Appl. Pharm. 224 (3) (2007) 241–248.

[44] H. Hennings, E.F. Spangler, R. Shores, P. Mitchell, D. Devor, A.K. Shamsuddin, et al., Malignant conversion and metastasis of mouse skin tumors: a comparison of SENCAR and CD-1 mice, Environ. Health Perspect. 68 (1986) 69–74.

[45] Z. Li, J. Huang, S. Shen, Z. Ding, Q. Luo, Z. Chen, et al., SIRT6 drives epithelial-to-mesenchymal transition and metastasis in non-small cell lung cancer via snail-dependent transrepression of KLF4, J. Exp. Clin. Cancer Res. 37 (1) (2018), 323.

[46] X.M. Li, S.J. Kim, D.K. Hong, K.E. Jung, C.W. Choi, Y.J. Seo, et al., KLF4 suppresses the tumor activity of cutaneous squamous cell carcinoma (SCC) cells via the regulation of SMAD signaling and SOX2 expression, Biochem Biophys. Res. Commun. 516 (4) (2019) 1110–1115.

[47] X. Zhang, R. Chen, L.D. Song, L.F. Zhu, J.F. Zhan, SIRT6 promotes the progression of prostate cancer via regulating the Wnt/β-catenin signaling pathway, J. Oncol. 2022 (2022), 2174758.

[48] J.S. Bae, S.J. Noh, K.M. Kim, S.H. Park, U.K. Hussein, H.S. Park, et al., SIRT6 is involved in the progression of ovarian carcinomas via β-catenin-mediated epithelial to mesenchymal transition, Front. Oncol. 8 (2018), 538.

[49] Y. Zhang, X. Wang, Targeting the Wnt/β-catenin signaling pathway in cancer, J. Hematol. Oncol. 13 (1) (2020), 165.